Turbulence in the near wake of a full-scale long-span bridge

Nicolò Daniotti[1,4], Jasna B. Jakobsen[1], Jonas T. Snæbjörnsson[1,2], Etienne Cheynet[3]

[1] Department of Mechanical and Structural Engineering and Materials Science, University of Stavanger, Stavanger, Norway. jasna.b.jakobsen@uis.no
[2] Department of Engineering, University of Reykjavík,Reykjavík, Iceland. jonasthor@ru.is
[3] Geophysical Institute and Bergen Offshore Wind Centre, University of Bergen, Bergen, Norway. etienne.cheynet@uib.no
[4] Svend Ole Hansen ApS, Copenhagen, Denmark. nid@sohansen.dk

Abstract

The present work introduces new measurement data on the interaction of natural wind with a closed box bridge girder, addressing a knowledge gap in full-scale bridge aerodynamics. The field measurements are performed at the Lysefjord Bridge wind and vibrations laboratory. Two dedicated sonic anemometers are installed in the proximity of the leading and trailing edge of the deck. The acquired wind turbulence data at the deck level is referenced to simultaneous observations of the incoming flow 6 m above the deck. The distortion of turbulent eddies on the upstream deck side is discussed, as well as the vortex-shedding process in the wake of the deck. As the prevailing wind directions are associated with a skew wind action on the bridge, a three-dimensional mean flow field around the bridge girder is captured by the anemometers and described in terms of mean and turbulent integral and spectral flow characteristics.

1 Introduction

For wind engineers, the full-scale measurement of the turbulent flow around a bridge girder is a unique opportunity to study bridge aerodynamics. Yet, such measurements remain exceptionally rare compared to wind tunnel tests or numerical models. Although lidar remote sensing has been used to explore the flow structure around bluff bodies (e.g. Cheynet et al., 2017), this technology is challenging to apply for small-scale turbulence measurements in the immediate vicinity of the bridge structure. In the present study, an array of 3D ultrasonic anemometers is deployed around a suspension bridge girder to study the vortex-shedding process and the distortion of the eddies upstream and downstream of the deck.

2 Instrumentation and method

The measurements are undertaken on the Lysefjord suspension bridge (58.9237°N 6.0985°E, fig. 1) crossing the inlet of a Norwegian fjord, which is a highly complex mountainous terrain. The bridge has a main span of 446 m, with its midspan located 55 m above the mean sea level. Wind flow from north-northeast or south-southwest is predominantly observed at the site (Cheynet et al., 2019).

The turbulent flow is studied around one cross-section of the deck, near hanger no. 08, which is on the Northern side of the bridge's main span. The instruments deployed on this location are summarized in table 1 and fig. 1.

Stationary velocity records with a duration of 20 min acquired during one year from 01/08/2020 to 01/08/2021 are selected. These events are associated with near-neutral atmospheric stability and a

Table 1. Instruments deployed near Hanger 08 of the Lysefjord Bridge since 2020-07.

Sensor name	Type	Brand
H08Wt	3D omnidirectional sonic anemometer	Gill Instrument
H08Wb	3D omnidirectional sonic anemometer	Gill Instrument
P08Wt	Pressure probe	Hoxey type (Moran & Hoxey, 1979)
P08Et	Pressure probe	Hoxey type (Moran & Hoxey, 1979)
D08E	3D asymmetric sonic anemometer	Gill Instrument
D08W	3D asymmetric sonic anemometer	Gill Instrument
P08W	Pressure probe	Hoxey type (Moran & Hoxey, 1979)
P08E	Pressure probe	Hoxey type (Moran & Hoxey, 1979)

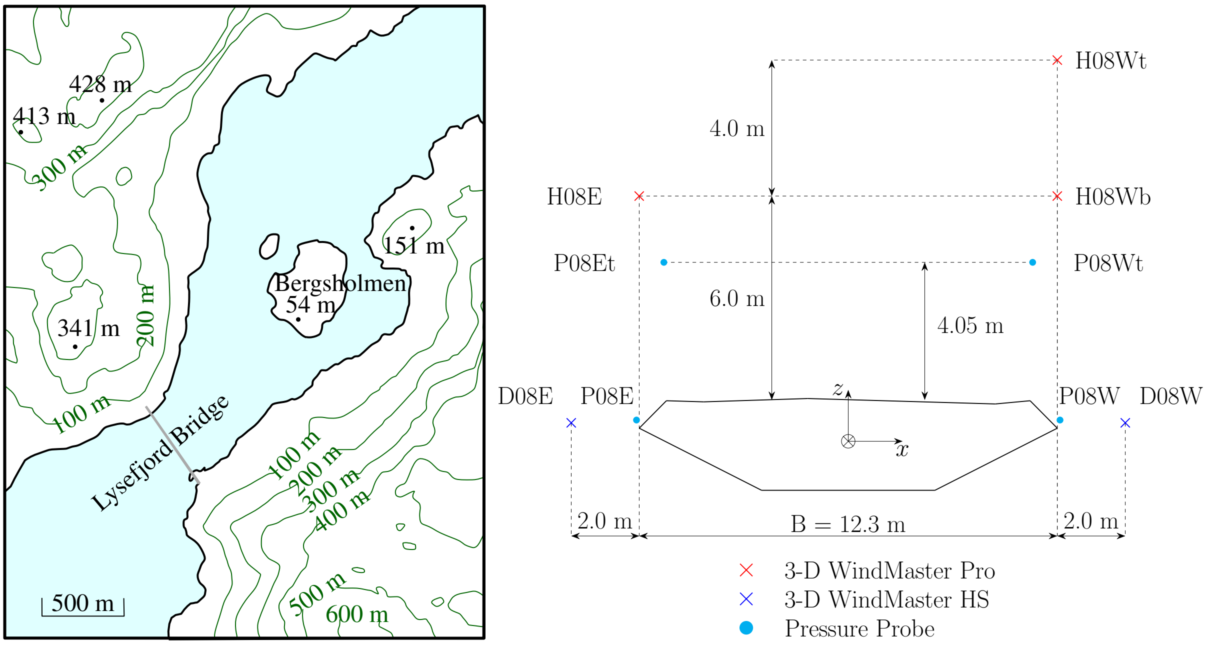

Figure 1. Topographic map of the area around the Lysefjord Bridge (left panel) and schematic of the deck cross-section of the Lysefjord Bridge where the instruments are deployed near hanger 08 (right panel).

north-northeast wind exposure, which leads to 219 samples. The thermal stratification of the atmosphere was estimated using the eddy covariance method and the 3D ultrasonic anemometer on H08E. Data with an absolute mean angle of attack above 10° or a mean wind speed under 6 m s^{-1} were dismissed.

The turbulent flow in the near wake of a bluff body can be highly three-dimensional. Thus, the turbulent flow is studied both in the traditional wind-based coordinate system (u, v, w) and in a deck-based coordinate system (v_x, v_y, v_z). Hereinafter, the v_x and v_y components are perpendicular and parallel to the main span axis, respectively, and v_z is the vertical velocity component.

Both integral and spectral characteristics of turbulence are studied. The velocity spectra are computed using Thomson (1982) multi-taper method, with a time-half bandwidth product of 4, and subsequently smoothed over 100 frequency windows, the centre of which is equally spaced along a logarithmic axis. The lowest frequency resolved is $1.7 \cdot 10^{-3}$ Hz. The normalization of each spectrum is based on the variance of the undisturbed turbulence, which is designated as $(\sigma^2_{v_z})_0$. Eventually, the ensemble average of the normalized power spectral densities is performed using the median operator for each normalized frequency bin.

3 Results

Figure 2 quantifies the relationship between the mean wind speed $\overline{u}$, the mean yaw angle β and the mean angle of wind incidence α recorded at H08E and D08E. On D08E, 2 m upstream of the deck leading edge, the mean velocity parallel to the (local) streamline decreases by 9%. This reflects the blocking by the bridge deck as the flow approaches the stagnation region, where the adverse pressure gradient is expected to be relatively strong (Bearman, 1972). Due to the asymmetry of the cross-section, the ratio $\overline{u}$(D08E)/$\overline{u}$(H08E) increases slightly as α decreases. The yaw angle β on D08E exhibits a systematic increase compared to the yaw angle estimated at H08E, thereby indicating that for $\beta \neq 0°$, the velocity component along the bridge axis increases locally. In other words, when the flow is at an angle, the streamlines deflect slightly towards the bridge axis as the stagnation region is approached. Finally, fig. 2 shows that flow 2 m upstream of the leading edge of the deck is deflected downwards. When $\alpha = 0°$ at H08E, the mean angle of wind incidence at D08E is $-7°$, which further reflects the three-dimensional flow distortion phenomenon.

As shown by fig. 3, the sonic anemometer on D08E records a significant increase in the vertical turbulence near the leading edge of the deck. Conversely, the standard deviation of the along-wind component is lower on D08E than on H08E. The spatial variation of the velocity components can be interpreted based on the theory developed by Hunt (1973) to describe the distortion of isotropic turbulence by a symmetrical bluff body. Following Hunt (1973), the mean and turbulent flow characteristics near the leading edge of the deck depend on the ratio L_u^x/D, where L_u^x is a length scale of turbulence and $D = 2.76$ m is the height of the bridge girder. When $L_u^x/D \gg 1$, as in the present case, a decrease of σ_u and $\overline{u}$ and an increase of σ_w is expected, in agreement with figs. 2 and 3.

The left panel of fig. 4 shows the ensemble-averaged normalised velocity spectra of v_z estimated in

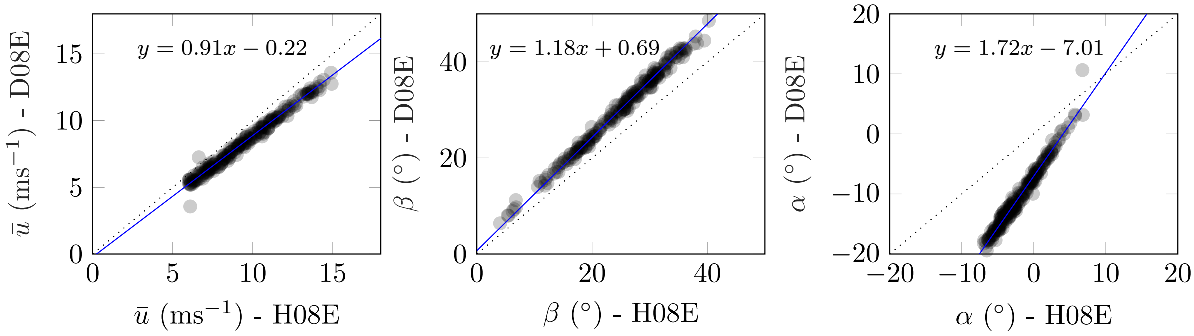

Figure 2. Relationship between mean wind speed $\overline{u}$ (left panel), mean yaw angle β (mid panel) and mean angle of wind incidence α (right panel) recorded by H08E and D08E (upstream of the deck).

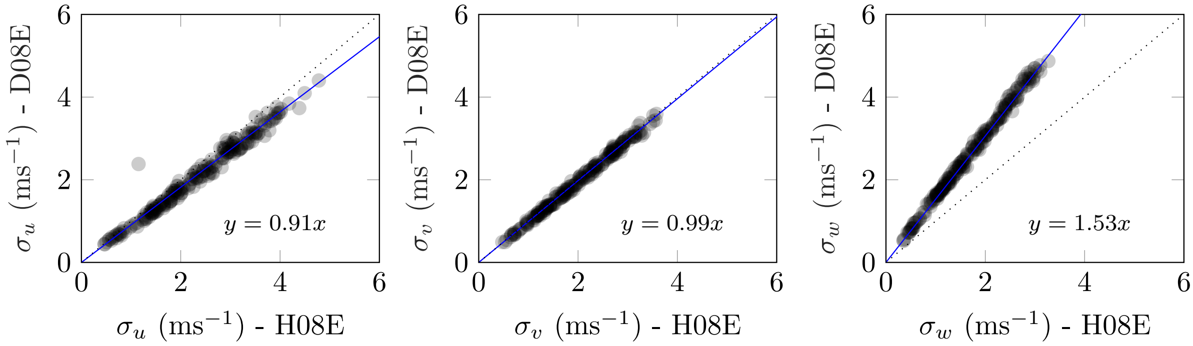

Figure 3. Relationship between σ_u (left panel), σ_v (mid panel) and σ_w (right panel) recorded by H08E and D08E (upstream of the deck).

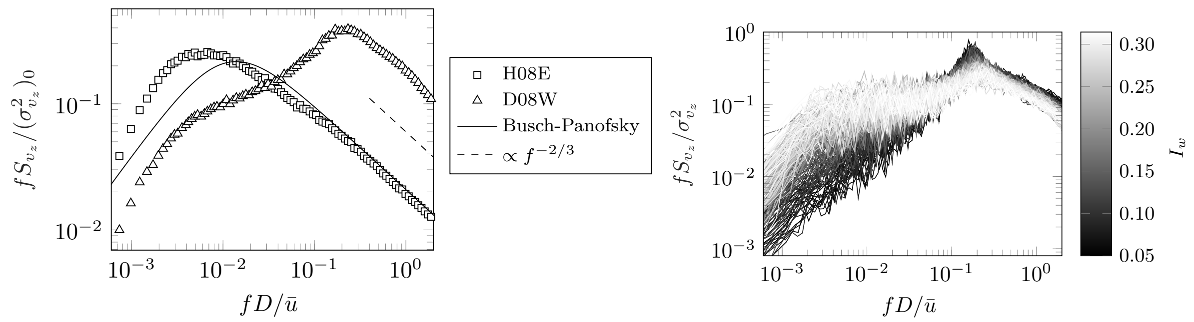

Figure 4. Left panel: Ensemble-averaged one-point velocity spectrum S_{v_z} in the near wake (D08W) for north-northeasterly flows with $u \geq 6\,\mathrm{m\,s^{-1}}$. The normalization is based on the variance of the (nominally) undisturbed turbulence measured by H08E. Right panel: Influence of incoming turbulence intensity (I_w) on the one-point velocity spectrum S_{v_z} in the near wake (D08W) for north-northeasterly flows.

the near wake region (D08W) and in the undisturbed region (H08E). For reference, the Busch-Panofsky spectrum (Busch & Panofsky, 1968) is superimposed on these spectra.

As seen in the left panel of fig. 4, the spectral energy is clearly affected by the presence of the bridge deck, which acts as a high-pass filter. Increasing the spectral energy at higher reduced frequencies and reducing it at lower reduced frequencies. For $f_r < 8 \cdot 10^{-3}$, eddies are significantly larger than the characteristic length D of the deck. Therefore, they may not be substantially affected by the bridge structure, as shown by the similar slope $\propto f^1$ for both velocity spectra upstream and downstream of the deck at low reduced frequencies. In the near wake, the fS_{v_z} spectrum peaks within a reduced frequency range centred at $f_r \approx 0.20$. This value corresponds to the median non-dimensional vortex shedding frequency, i.e. the Strouhal number St associated with the studied bridge deck.

The right panel of fig. 4 shows how the shape of the S_{v_z} spectrum in the near wake region is influenced by the vertical turbulence intensity I_w. This reflects the fact that high turbulence prevents the existence of a narrow-banded vortex-shedding process. For $I_w < 0.10$, the narrow peak at $f_r \approx 0.20$ reflects the aforementioned St number of the bridge deck.

4 Conclusions

This paper investigates full-scale wind turbulence near the leading and trailing edges of the Lysefjord bridge deck. North-easterly stationary wind velocity records representative of a near-neutral atmosphere were acquired over one year. The paper provides valuable findings relevant to the aerodynamics of yawed line-like sharp-edged bodies.

The Sonic anemometry is effective in monitoring the vortex formation on the leeward side of a prototype bridge deck. Complementary hot-wire measurements undertaken in the near wake of a 1:50 stationary sectional model are available and provide insight into the potential sensitivity of the Strouhal number on the Reynolds number effects. The significance of a skewed incident flow on the near-wake topology will also be discussed based on a related wind tunnel study.

The time-averaged wind characteristics were estimated at 0.74D from the trailing edge. They revealed a pronounced axial flow when the oncoming flow is skewed more than 15°. The vertical velocity fluctuations were proven to be an effective indicator of the vortex-shedding process. The Strouhal number estimates were found fairly sensitive to the turbulence intensity in the approaching flow. The higher the turbulence intensity, the higher the Strouhal number. Its median value was found to be 0.20.

Acknowledgments

The support of the Norwegian Public Roads Administration for the monitoring project on the Lysefjord Bridge and Svend Ole Hansen ApS for performing the wind tunnel tests designed by the UiS team is greatly acknowledged.

References

Bearman, P. (1972). Some measurements of the distortion of turbulence approaching a two-dimensional bluff body. *Journal of Fluid Mechanics*, **53**, 451–467.

Busch, N. E., & Panofsky, H. A. (1968). Recent spectra of atmospheric turbulence. *Quarterly Journal of the Royal Meteorological Society*, **94**, 132–148.

Cheynet, E., Jakobsen, J. B., & Snæbjörnsson, J. (2019). Flow distortion recorded by sonic anemometers on a long-span bridge: Towards a better modelling of the dynamic wind load in full-scale. *Journal of Sound and Vibration*, **450**, 214–230.

Cheynet, E., Jakobsen, J. B., Snæbjörnsson, J., Angelou, N., Mikkelsen, T., Sjöholm, M., & Svardal, B. (2017). Full-scale observation of the flow downstream of a suspension bridge deck. *Journal of Wind Engineering and Industrial Aerodynamics*, **171**, 261–272.

Hunt, J. (1973). A theory of turbulent flow round two-dimensional bluff bodies. *Journal of Fluid Mechanics*, **61**, 625–706.

Moran, P., & Hoxey, R. (1979). A probe for sensing static pressure in two-dimensional flow. *Journal of Physics E: Scientific Instruments*, **12**, 752.

Thomson, D. J. (1982). Spectrum estimation and harmonic analysis. *Proceedings of the IEEE*, **70**, 1055–1096.